

EFFECT OF INCLINED MAGNETIC FIELD ON THE OSCILLATORY FLOW OF MICROPOLAR FLUID IN A POROUS MICRO-CHANNEL UNDER THE ACTION OF ALTERNATING ELECTRIC FIELD.

Ajaz Ahmad Dar^{1*} and K. Elangovan²

¹Department of Mathematics, Annamalai University, Annamalainagar - 608 002, India.

²Mathematics Section, FEAT, Annamalai University, Annamalainagar - 608 002, India.

Article Received on 05/11/2016

Article Revised on 25/11/2016

Article Accepted on 15/12/2016

***Corresponding Author**

Ajaz Ahmad Dar

Department of
Mathematics, Annamalai
University,
Annamalainagar - 608 002,
India.

ABSTRACT

Electroosmotic flows of micropolar fluids in microchannel are of great significance due to their manifold applications in the transport of liquids, mainly when the ionized liquid flows with regard to a charged surface in the presence of an alternating electric field. This article presents a complete theoretic study on the electro-osmotic flow of a micropolar fluid in a porous microchannel. The effect of the inclined

magnetic field and electro-osmotic parameters on the kinematics of the fluid is taken into consideration. The analytical expressions of the electro-osmotic velocity and the microrotation of the suspended microparticles are derived within the framework of the Debye-Huckel Approximation. A quantitative study has been made through numerical calculation of the physical variables associated with the electro-osmotic flow of a micropolar fluid. This study provides a basis of novel understanding into the process of designing bio-detecting and micro-fluidic devices. It will also be important in the development of nano-scale bio-sensor advances as well as mechanical and electrical transducer components.

KEYWORDS: Electro-osmotic flow, Debye-Huckel parameter, inclined magnetic field, micropolar fluid, Electrical double layer.

1. INTRODUCTION

In recent years, microfluidics has appeared as a fundamental branch of fluid mechanics. It has

been receiving growing interest in scientific research and has manifold applications not only in engineering and technology, but also in various branches of science, including physiological and medical sciences. Investigation on electroosmotic flow in micro-channels has occupied central position in scientific research. Renewed interests with fast and thriving development of BioMENS and Lab-on-a-chip technologies due to its powerful activation mechanism to manipulate liquid samples of nano-volumes in capillary network of these devices.

In recent investigation by Misra et al.^[1], it has been declared that when an electrolytic liquid comes in contact with a solid surface, an Electrical Double Layer (EDL) is formed in the inter-facial region. The Electrical Double Layer comprises a layer of charges of one polarity on the solid side and a layer of charges of opposite polarity on the liquid side of the solid-liquid interface. This phenomenon was mostly attributed to the contribution of Helmholtz. In order to resolve problems arising because of highly charged double layers, Stern suggested the concentration of an additional internal layer, called the Stern Layer, where the ions are strongly bound. Rice and Whitehead^[2] used Debye Huckel linearization for investigating fully developed electroosmotic flow in a narrow cylindrical capillary for low zeta potentials. Kang et al.^[3] studied the analytical solution for electroosmotic flow in a cylindrical capillary by solving the complete Poisson-Boltzmann equation for arbitrary zeta potentials. Misra and Chandra^[4] investigated the electroosmotic flow of a second-grade fluid in a porous microchannel under the action of an alternating electric field. Electroosmotic flow and heat transfer of a non-Newtonian fluid in a hydrophobic microchannel with Navier slip has been studied by Misra and Sinha.^[5] They observed that Joule heating has a dominant role to play in controlling the temperature of blood in micro-vessels of the circulatory system. Wooseok Choi et al.^[6] studied electroosmotic flows of viscoelastic fluids with asymmetric electrochemical boundary conditions by using Phan-Thien Tanner (PTT) constitutive model. Matios et al.^[7] presented an analytical model that examines the influence of Joule heating on the slip velocity in an electroosmotic flow (EOF) of viscoelastic fluid. Analytical model that describes a two-fluid electroosmotic flow of stratified fluids with Newtonian or viscoelastic rheological behavior has been described by Afonso et al.^[8] Cunlu Zhao and Chun Yang^[9] studied transient electroosmotic flow of viscoelastic fluids in rectangular microchannels. Further, they investigated the exact solution for electroosmosis of non-newtonian fluids in microchannels.^[10] Moreover, several investigators studied electroosmotic flows in microchannels under different conditions.^{[11]-[19]}

So far, many non-newtonian fluid models have been proposed. The effect of rotation of the microparticles of the fluid requires more attention of the investigators. The microrotation of the particles bears the potential to affect the behavior of the fluid flow, mainly in the case of fluid flow in microchannels. Now-a-days the theory of micropolar fluids proposed by Erigen^{[20]-[21]} has received a great attention in the scientific research because of its wide range of applications in many research areas. Micropolar fluids exhibit couple stresses, and in addition to the velocity vector the particles of the fluid have an independent rotation vector. Many fluids, such as blood, polymeric suspensions and liquid crystals can be treated as micropolar fluids.^[22] Modeling complex flows as micropolar fluids, Papautsky et al.^[29] illustrated that the micropolar fluid model might provide better convention with the experimental data for microfluidic devices than the Newtonian fluid theory. Magyari et al.^[30] examined the first Stokes problem for a micropolar fluid. Further reviews of the polar fluid theory and its applications can be found in Refs.^{[31]-[35]}

The theoretical study of the electroosmotic flows of micropolar fluids is recent and rare, particularly for the time-dependent Electroosmotic flows. Siddiqui and Lakhtakia^{[23]-[24]} studied some boundary value problems of one-dimensional electroosmotic symmetric channel flow of a micropolar fluid. Misra et al.^[25] observed the electroosmotic flow of a physiological fluid with prominent micropolar characteristics. Misra et al.^[26] studied the electroosmotic flow of a micropolar bio-fluid between two plates that are in the state of periodic vibrations. Moreover, Zhaodong Ding et al.^[27] studied the time periodic electro-osmotic flow of an incompressible micropolar fluid through micro-parallel channel. Siddiqui and Lakhtakia^[28] obtained Debye Huckel solution for steady electro-osmotic fluid in a cylindrical microcapillary.

Most of the studies on electroosmotic flow have been observed for the cases when the system is under the action of DC electric field. But the DC electric field can never fulfill the requirements of different suitable large voltages keeping at par with biological samples. Electroosmosis arising out of DC electric field is the main cause of the bubble formation which is another drawback of the DC electric field. Keeping in mind, the importance of electroosmotic flow subject to an alternating electric field and its enormous applications in engineering, medical science and separation science, an attempt has been made to analyze the effect of inclined magnetic field on the micropolar fluid in a porous microchannel subject to an AC electric field. This study will serve to understand the actual physics of the problem and

the influence of various physical parameters involved in it. To examine the validity of the present analysis to the biological science, the computational work has been observed and performed by considering blood as a micropolar fluid. Debye Huckel Approximations have been used to obtain the analytical solutions of axial velocity and microrotation.

2. Mathematical Formulation

To begin with, let us consider the Cartesian coordinate system described in Figure 1. The motion of a viscous incompressible ionized micropolar fluid through a microchannel between two oscillatory porous plates located at $y = \pm h$ will be analyzed here subject to an alternating electric field of strength E . A uniform magnetic field of strength B_0 is applied at an angle of Θ to the y axis. Suppose that the fluid flows in the direction of x -axis of the channel with a velocity u expressed as $u = u(y, t)$. Then, the continuity equation reduces to $\frac{\partial u}{\partial x} = 0$. Assuming that the flow is symmetric about the axis $y = 0$, we can restrict our study to the region $0 \leq y \leq h$ only. The height of the microchannel is $2h$. The applied electric field E is parallel to the x -axis, and is spatially uniform within the microchannel. With these considerations, our specific concern is to examine various significant features of the electroosmotic flow, where the system is under the action of an alternating electric field.

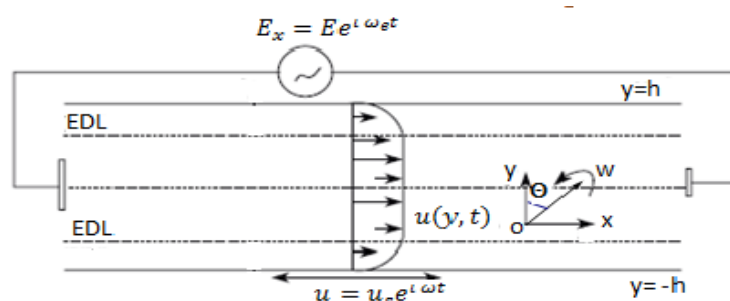


Figure 1: Geometry of the Problem.

Generally, the Reynolds number is low for the flow in a microchannel. Therefore, the inertial force is very small as compared to the viscous force. Hence in the present problem we can ignore the nonlinear inertial term in the governing equation of motion. Though, the unsteady inertial factor that represents the acceleration of the flow will be taken into account. Under the aforesaid considerations and applying boundary layer approximations, the system of equations governing the unsteady time-periodic electro-osmotic fully developed flow of the micropolar fluid are given by

$$\frac{\partial u}{\partial t} = -\frac{1}{\rho} \frac{\partial p}{\partial x} + \left(\nu + \frac{k}{\rho} \right) \frac{\partial^2 u}{\partial y^2} + \frac{k}{\rho} \frac{\partial w}{\partial y} - \frac{\sigma B_0^2}{\rho} \cos^2 \Theta (u) - \frac{\nu}{K_1} u + ac\rho_s \rho E_x e^{i\omega_s t}. \quad (1)$$

$$\frac{\partial w}{\partial t} = \frac{\gamma_s}{\rho_j} \frac{\partial^2 w}{\partial y^2} - \frac{k}{\rho_j} \left(2w + \frac{\partial u}{\partial y} \right). \quad (2)$$

The charge density ρ_s and the electric potential ψ are related by Gauss's law of charge distribution and is given below

$$\frac{d^2 \psi}{dy^2} = -\frac{\rho_s}{\epsilon} \quad (3)$$

Where $\rho_s = -2n_0 e z \sinh \left(\frac{ez\psi}{K_B T} \right)$ represents the distribution of net electric charge density in equilibrium near a charged surface, w signifies the microrotation describing the micropolar behavior of the fluid, which gives a measure of the rotating velocity of the rigid/semi-rigid particles of the fluid about their respective centroids, ϵ is the dielectric constant of the electrolyte liquid, n_0 is the ion density of the bulk liquid, ω is the angular velocity of oscillation of the channel walls, z is the valence, K_B is the Boltzmann constant, e is the electron charge, k stands for the vortex viscosity, t for time variable, T for absolute temperature and ρ for fluid density. E is the externally applied electric field, B_0 is the strength of the externally applied magnetic field, Θ is the inclination angle of the magnetic field and K_1 is the permeability parameter. The symbol γ_s denotes the spin gradient viscosity and is given by.

$$\gamma_s = \left(\mu + \frac{k}{2} \right) j = \mu \left(1 + \frac{K}{2} \right) j \quad (4)$$

where $K = \frac{k}{\mu}$ represents the micropolar fluid parameter. Now we introduce the non-dimensional variables and parameters defined as.

$$x' = \frac{x}{h}, \quad y' = \frac{y}{h}, \quad u' = \frac{u}{U_{HS}}, \quad t' = \frac{t U_{HS}}{h}, \quad p' = \frac{ph}{\mu U_{HS}}, \quad w' = \frac{wh}{U_{HS}},$$

$$H_a = \sqrt{\frac{\sigma}{\mu}} h B_0, \quad R_s = \frac{U_{HS} h}{\nu}, \quad \omega' = \frac{\omega h}{U_{HS}}, \quad \omega'_s = \frac{\omega_s h}{U_{HS}}, \quad \psi' = \frac{\psi}{\zeta}, \quad K_1 = \frac{K_1}{h^2} \quad (5)$$

We have used $j = h^2$ as a micro-inertia parameter per unit mass. H_a is the Hartmann number and U_{UHS} is the unsteady Helmholtz-Smoluchowski electro-osmotic velocity which is defined as.

$$U_{UHS} = U_{HS} e^{i\omega t} = -ME = \frac{-\zeta E e^{i\omega t}}{\mu} \quad (6)$$

where M denotes the measure of the mobility of ions in the ionized state of the fluid, ζ represents the zeta potential, and $\mu = \rho\nu$ is the dynamic viscosity of the fluid.

Using the above mentioned non-dimensional variables, we can rewrite the Equations (1), (2) and (3) in the modified form as.

$$R_s \frac{\partial u'}{\partial t'} = -\frac{\partial p'}{\partial x'} + (1+K) \frac{\partial^2 u'}{\partial y'^2} + K \frac{\partial w'}{\partial y'} - H_a^2 \cos \Theta (u') - \frac{1}{K_1} u' + \frac{\partial^2 \psi'}{\partial y'^2} e^{i\omega' t'}. \quad (7)$$

$$R_s \frac{\partial w'}{\partial t'} = \left(1 + \frac{K}{2}\right) \frac{\partial^2 w'}{\partial y'^2} - K \left(2w' + \frac{\partial u'}{\partial y'}\right). \quad (8)$$

and

$$\frac{d^2 \psi'}{dy'^2} = \frac{2n_0 e z h^2}{\zeta} \sinh \left(\frac{e z \zeta}{K_B T} \psi' \right) \quad (9)$$

Under the scope of standard kinetic theory conditions, since the electric potential energy is small as compared to the thermal energy of the ions so that^[36]

$$|e z \zeta \psi'| < |K_B T|$$

Then Equation (9) reduces to

$$\frac{d^2 \psi'}{dy'^2} = m^2 \psi' \quad (10)$$

where m is called the Debye-Huckel parameter (in the non-dimensional form) and is defined by

$$m^2 = \frac{h^2}{\lambda^2} = \frac{2n_0 e^2 z^2 h^2}{K_B T}$$

λ being the thickness of the Debye layer.

The solution of Equation (10) subject to the boundary conditions

$$\psi'(0) = 0, \quad \psi'(\pm 1) = 1 \quad \text{and} \quad \left(\frac{d\psi'}{dy'} \right)_{y'=0} = 0 \quad (11)$$

is given by

$$\psi'(y') = \frac{\cosh(my')}{\cosh(m)} \quad (12)$$

In the sequel, we shall drop the superscript “'” to give a more appropriate look to the equations containing non-dimensional variables. We shall consider

$$u = u_s e^{i\omega t}, \quad w = w_s e^{i\omega t}, \quad \frac{\partial p}{\partial x} = \phi e^{i\omega t} \quad (13)$$

where u_s and w_s represents the steady part of the axial velocity and spin velocity respectively.

Making use of Equations. (12) and (13) in Equations. (7) and (8), we get the following equations

$$\frac{\partial^2 u_s}{\partial y^2} + \left(\frac{K}{1+K} \right) \frac{\partial w_s}{\partial y} = -\frac{\phi}{1+K} - n^2 u_s + \frac{m^2 \cosh(my)}{(1+K) \cosh(m)} = 0 \quad (14)$$

$$\left(\frac{2+K}{2K} \right) \frac{\partial^2 w_s}{\partial y^2} - l^2 w_s - \frac{\partial u_s}{\partial y} = 0 \quad (15)$$

$$\text{where } n^2 = \frac{R_s i\omega + H_a^2 \cos^2 \theta + \frac{1}{K_1}}{1+K} \text{ and } l^2 = \frac{i\omega R_s + 2K}{K}$$

The boundary conditions for the velocity and microrotation of the microparticles can be written in the form:

$$\frac{\partial u_s}{\partial y} = 0, \quad w_s = 0 \quad (16)$$

$$u_s = u_0, \quad w_s = \beta \frac{\partial u_s}{\partial y} \quad (17)$$

3. Solution of the Problem

Differentiating Equation (15) with respect to y , we have

$$\frac{\partial^2 u_s}{\partial y^2} = \left(\frac{2+K}{2K} \right) \frac{\partial^3 w_s}{\partial y^3} - l^2 \frac{\partial w_s}{\partial y} \quad (18)$$

By substituting Equation (18) into Equation (14) and solving, we arrive at

$$u_s = A_3 \frac{\partial^3 w_s}{\partial y^3} - A_1 \frac{\partial w_s}{\partial y} + B + A_2 \cosh(my) \quad (19)$$

$$\text{where } A_1 = \frac{l^2(1+K)-K}{n^2(1+K)}, \quad A_2 = \frac{m^2}{n^2(1+K) \cosh(m)}, \quad A_3 = \frac{2+K}{2Kn^2}, \quad B = \frac{-\phi}{n^2(1+K)}$$

Differentiating Equation (19) and then using the obtained result in Equation (15), we get

$$\frac{\partial^4 w_s}{\partial y^4} - A_4 \frac{\partial^2 w_s}{\partial y^2} + A_5 w_s + A_6 \sinh(my) = 0 \quad (20)$$

$$\text{where } A_4 = \frac{2KA_1 + 2 + K}{2KA_3}, \quad A_5 = \frac{l^2}{A_3}, \quad \text{and } A_6 = \frac{mA_2}{A_3}$$

whose general solution is

$$w_s = C_1 e^{-yR_1} + C_2 e^{yR_1} + C_3 e^{-yR_2} + C_4 e^{yR_2} + A_7 \sinh(my) \quad (21)$$

$$\text{where } R_1 = \frac{\sqrt{A_4 - \sqrt{A_4^2 - 4A_5}}}{\sqrt{2}}, R_2 = \frac{\sqrt{A_4 + \sqrt{A_4^2 - 4A_5}}}{\sqrt{2}}, A_7 = \frac{4A_6}{(2m^2 - A_4 + \sqrt{A_4^2 - 4A_5})(-2m^2 + A_4 + \sqrt{A_4^2 - 4A_5})}$$

Substituting Equation (21) into Equation (19), we get

$$u_s = C_1 A_8 e^{-yR_1} - C_2 A_8 e^{yR_1} + C_3 A_9 e^{-yR_2} - C_4 A_9 e^{yR_2} + A_{10} \cosh(my) + B \quad (22)$$

where

$$A_8 = -A_3 R_1^3 + A_1 R_1 \quad (23)$$

$$A_9 = -A_3 R_2^3 + A_1 R_2 \quad (24)$$

$$A_{10} = A_3 A_7 m^3 - A_1 A_7 m + A_2 \quad (25)$$

The values of C_1, C_2, C_3 and C_4 can be found by applying the boundary conditions from Equations (16) and (17) into Equations (21) and (22) and are calculated as

$$C_1 = -C_2 = -\frac{A_{11} A_7 A_9 + m\beta A_{11} A_9 A_{10} - \sinh(R_2)(1 + \beta A_9 R_2)(B + \cosh(m)A_{10} - u_0)}{2 \cosh(R_2) \sinh(R_1) A_9 (1 + \beta A_8 R_1) - 2 \cosh(R_1) \sinh(R_2) A_8 (1 + \beta A_9 R_2)} \quad (26)$$

$$C_3 = -C_4 = \frac{A_{12} A_7 A_8 + m\beta A_{12} A_8 A_{10} - \sinh(R_1)(1 + \beta A_8 R_1)(B + \cosh(m)A_{10} - u_0)}{2 \cosh(R_2) \sinh(R_1) A_9 (1 + \beta A_8 R_1) - 2 \cosh(R_1) \sinh(R_2) A_8 (1 + \beta A_9 R_2)} \quad (27)$$

where

$$A_{11} = \cosh(R_2) \sinh(m)$$

$$A_{12} = \cosh(R_1) \sinh(m)$$

Equations (21) and (22) provide the required solution for the steady part of the microrotation of the microparticles and electro-osmotic flow velocity respectively, while for the problem under consideration at any instant, the microrotation of the fluid particles is given by $w = w_s e^{i\omega t}$ and the axial velocity is given by $u = u_s e^{i\omega t}$.

The volumetric flow rate is then given by

$$Q = 2 \int_0^1 u(y, t) dy = 2Q_0 e^{i\omega t} \quad (28)$$

where

$$Q_0 = \int_0^1 u_s(y) dy = \frac{A_8}{R_1} \{C_1(1 - e^{-R_1}) - C_2(-1 + e^{R_1})\} + \frac{A_9}{R_2} \{C_3(1 - e^{-R_2}) - C_4(-1 + e^{R_2})\} + \frac{A_{10} \sinh(my)}{m} + B \quad (29)$$

4. RESULTS AND DISCUSSION

In this section, we intend to find numerical estimations of the electro-osmotic velocity of biological fluids (e.g., blood) in micro-bio-fluidic devices and also microrotation of microparticles (e.g., erythrocytes), by using the analytical expressions derived in Section 3. The computational work has been completed by using the software MATHEMATICA. The ranges of variation for the parameters β , m and K have taken to be $[-1,0]$, $[1,80]$ and $[2,8]$ respectively. Approximation of the physical variables has been made by taking $u_0 = 0.2$ and $\phi=10$, while other parameters are varied over a range and are given in the caption of the figures.

Fig.2 illustrates the variation of the velocity distribution with respect to y for different values of various embedded physical parameters. From Fig. 2(a), it is observed that with increasing magnitude of the magnetic field (i.e. increasing Hartmann number), the flow velocity gradually decreases due to the detrimental effect of the electromagnetic body force. Moreover, for higher values of H_a , the reduction in the flow velocity is more significant near the center of the capillary rather than near the wall. Fig. 2(b) illustrates that the value for the velocity u , is reduced with the enhancement of micropolar parameter K . Fig. 2(c) illustrates the variation of the velocity distribution in the lower range of the Reynolds number R_g . It is observed that with an increase in the Reynolds number R_g , the velocity of blood in a micro channel decreases. From Fig. 2(d), it is observed that the velocity increases with an increase in porous parameter K_1 . The shape factor of porous medium is the ratio between the permeability coefficient and the square of the height of the channel. So, any increase in the porous medium permeability coefficient causes a rise in the velocity of the fluid (blood). Fig. 2(e) illustrates the variation in the distribution of velocity u , in the case of steady electro-osmotic flow of micropolar fluid (blood) for different values of the Debye-Huckel Parameter m . The enhancement of blood velocity with the increase in m indicates that the variation in velocity with the increase in the height of the microchannel resembles similar effects in the case of a Newtonian fluid. It is also observed that the velocity gradient is higher in the mid-channel and gradually decreases as we move from the mid-channel to the boundary. of the channel. Fig. 2(f) illustrates the variation of velocity with different values of β . The parameter β is a constant related to the occurrence of electroosmosis, and it is considered as the boundary parameter. The velocity increases by increasing the magnitude of the boundary parameter β . This result is in good agreement with.^[23] From Fig. 2(g), it is depicted that by increasing the inclination angle θ of the magnetic field, the velocity of the fluid increases.

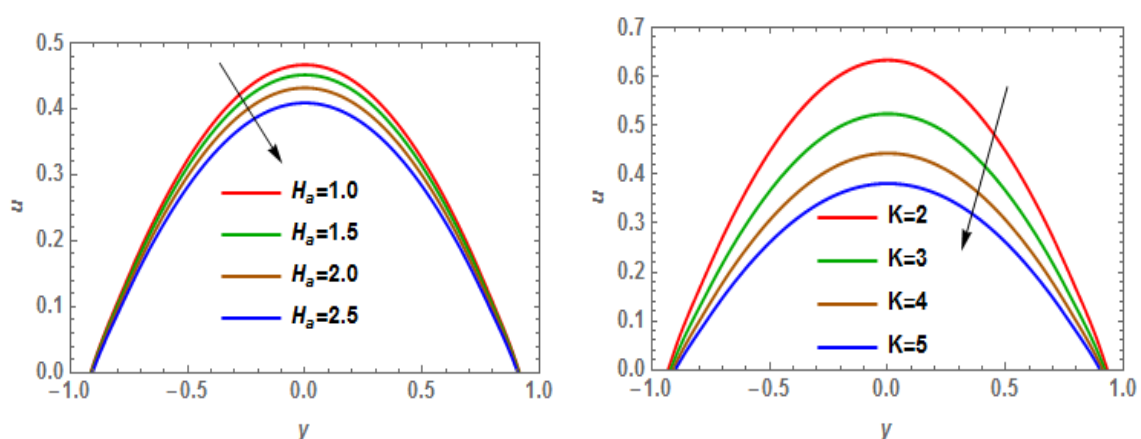
Fig. 3 displays the variation of the velocity with respect to t for different values of physical parameters involved in the analysis. From Fig. 3(a), it is observed that with increasing magnitude of the magnetic field (i.e. increasing Hartmann number), the amplitude of the oscillation decreases. A similar trend is followed by the Reynolds number R_e and micropolar fluid parameter K as illustrated in Fig. 3(b) and Fig. 3(c). Fig. 3(d) illustrates that the amplitude of oscillation of blood velocity u increases as the value of the porous parameter K_1 is enhanced. Fig. 3(e) gives the variation in the blood velocity u near the wall ($y=0.9$) with change in the value of Debye-Huckel parameter m . It is observed that the amplitude of oscillation gets enhanced as the value of the Debye-Huckel parameter m increases. Since the Debye-Huckel parameter m increases with the increase in the width of the channel, it follows that the rise in the height of the micro-channel in relation to the Debye length causes amplification in the amplitudes of oscillation of the velocity. Fig. 3(f) reveals that the velocity increases by increasing the magnitude of the boundary parameter β . From Fig. 3(g), it is observed that there occurs negligible increase in the velocity by increasing the inclination angle of the magnetic field.

Fig. 4 displays the variation of microrotation of the microparticles (e.g., erythrocytes) with respect to y for different values of physical parameters of interest. The microrotation gradient is higher in the vicinity of the wall rather than in the mid-channel. Fig. 2(a-c) reveals that the microrotation of the erythrocytes decreases by increasing the values of Hartmann number H_a , Reynolds number R_e and micropolar fluid parameter K . The decreasing trend in microrotation with the increase in micropolar parameter, as depicted in Fig. 2(c) is in good agreement with that reported by Siddiqui and Lakhtakia.^[23] From Fig. 2(d-f), it is observed that the increasing values of boundary parameter β , porous parameter K_1 and Debye-Huckel parameter m , leads to an enhancement in the microrotation of the microparticles. Furthermore, the microrotation of the erythrocytes also increases by increasing the inclination angle Θ of the magnetic field as observed in Fig. 2(g).

Fig. 5 depicts the variation of the microrotation of the microparticles with respect to t for different values of physical parameters. From Fig. 5(a), it is observed that with increasing magnitude of the magnetic field (i.e. increasing Hartmann number), the amplitude of the oscillation decreases. From Fig. 5(b) and Fig. 5(c) it is observed that the effect of Reynolds number R_e and micropolar fluid parameter K on the microrotation is similar to the magnetic

field parameter. Fig. 5(d) illustrates that the amplitude of oscillation of microrotation w increases as the value of the porous parameter K_1 is enhanced. The spin velocity increases by increasing the magnitude of the boundary parameter β as depicted in Fig. 5(e). Fig. 3(f) gives the variation in the microrotation w near the wall ($y=0.9$) with change in the value of Debye-Huckel parameter m . It is observed that the amplitude of oscillation gets enhanced as the value of the Debye-Huckel parameter m increases. Since the Debye-Huckel parameter m increases with the increase in the width of the channel, it follows that the rise in the height of the micro-channel in relation to the Debye length causes amplification in the amplitudes of oscillation of the microrotation. From Fig. 3(g), it is observed that there occurs negligible increase in the microrotation of the microparticles by increasing the inclination angle Θ of the magnetic field.

The variation of the Volumetric Flow Rate Q with respect to t for different values of physical parameters is illustrated in Fig. 6. The variations of the amplitude of the normalized volume flow rate Q with H_a , R_e and K are presented in Fig. 6(a-c). It is observed that the volume flow rate decreases by increasing the magnetic field intensity, Reynolds number and micropolar fluid parameter. While the increasing values of K_1 , β and m show opposite trend as compared to the magnetic field parameter i.e. by increasing the values of porous parameter K_1 , boundary parameter β and Debye-Huckel parameter m , the amplitude of volume flow rate increases as displayed in Fig. 6(d-f). From Fig. 6(g), a negligible increase in the volume flow rate is observed when the inclination angle of the magnetic field is increased.



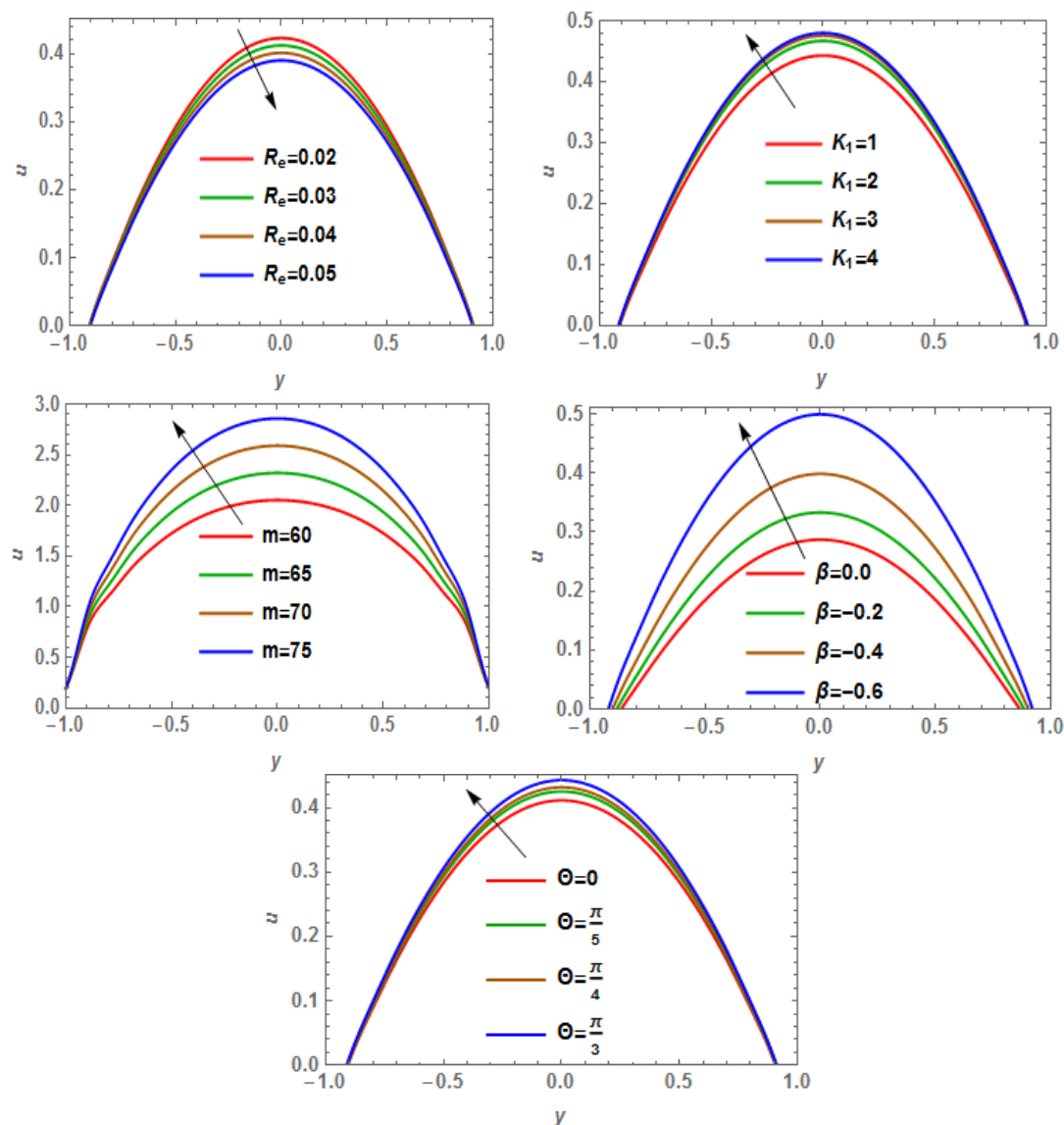


Figure 2(a-g). Velocity profile with respect to y for

- (a) $m = 3, \lambda = 10, \Theta = \frac{\pi}{3}, K = 4, t = 0.2, \beta = -0.5, u_0 = 0.2, R_e = 0.001, \omega = 10, K_1 = 2$;
- (b) $m = 3, \lambda = 10, \Theta = \frac{\pi}{3}, H_a = 1, t = 0.2, \beta = -0.5, u_0 = 0.2, R_e = 0.001, \omega = 10, K_1 = 1$;
- (c) $m = 3, \lambda = 10, \Theta = \frac{\pi}{3}, K = 4, t = 0.2, \beta = -0.5, u_0 = 0.2, H_a = 1, \omega = 10, K_1 = 1$;
- (d) $m = 3, \lambda = 10, \Theta = \frac{\pi}{3}, K = 4, t = 0.2, \beta = -0.5, u_0 = 0.2, R_e = 0.001, \omega = 10, H_a = 1$;
- (e) $H_a = 1, \lambda = 10, \Theta = \frac{\pi}{3}, K = 4, t = 0.2, \beta = -0.5, u_0 = 0.2, R_e = 0.001, \omega = 10, K_1 = 2$;
- (f) $m = 3, \lambda = 10, \Theta = \frac{\pi}{3}, K = 4, t = 0.2, H_a = 1, u_0 = 0.2, R_e = 0.001, \omega = 10, K_1 = 2$;
- (g) $m = 3, \lambda = 10, H_a = 1, K = 4, t = 0.2, \beta = -0.5, u_0 = 0.2, R_e = 0.001, \omega = 10, K_1 = 1$.

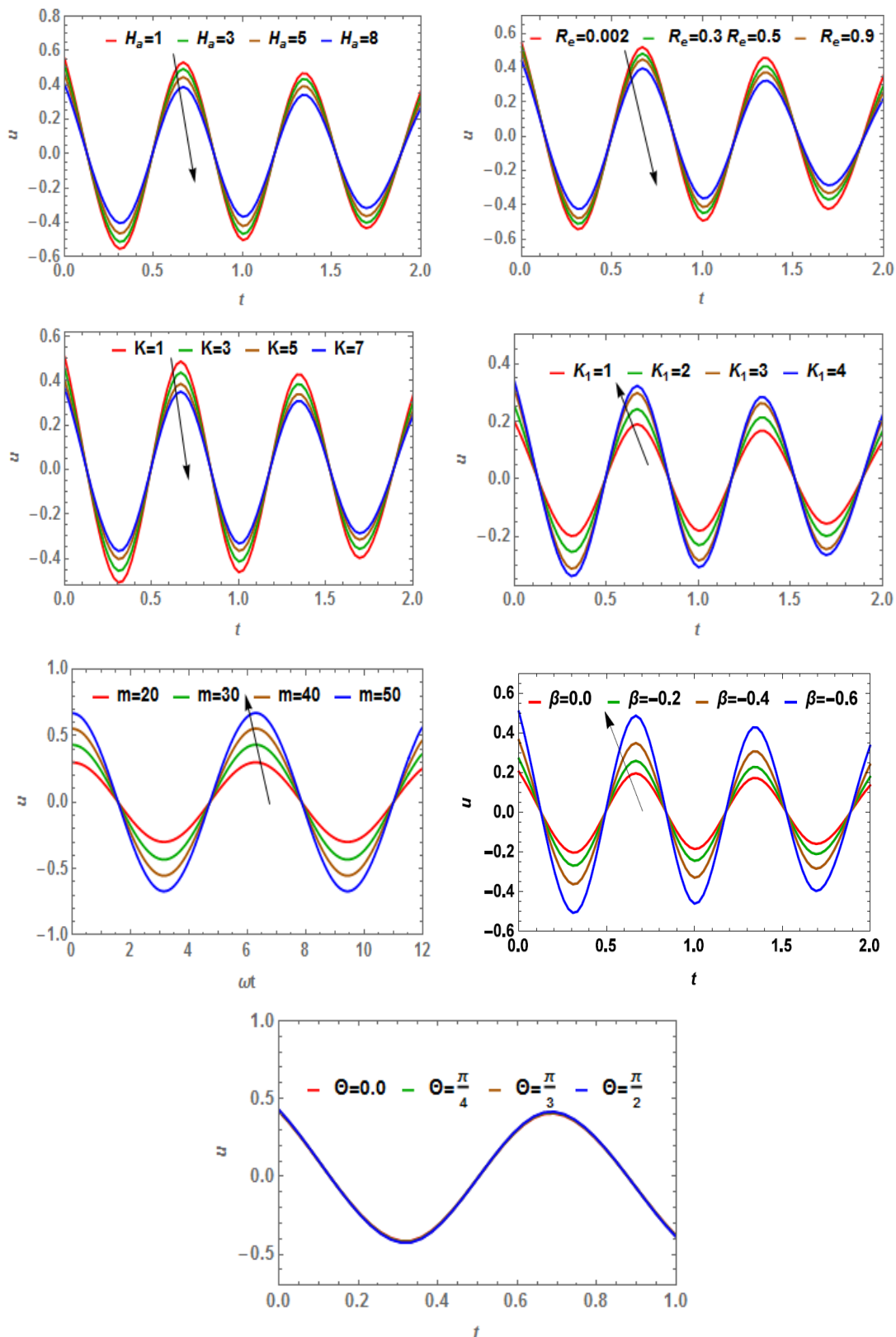


Figure 3(a-g). Velocity profile with respect to t for

(a) $m = 40, \lambda = 10, \Theta = \frac{\pi}{3}, K = 4, y = 0.9, \beta = -0.5, u_0 = 0.2, R_e = 0.001, \omega = 10, K_1 = 2;$

(b) $m = 40, \lambda = 10, \Theta = \frac{\Pi}{3}, K = 4, H_a = 1, y = 0.9, \beta = -0.5, u_0 = 0.2, \omega = 10, K_1 = 1$;

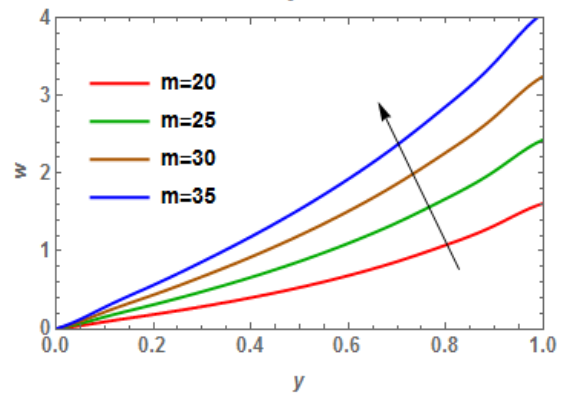
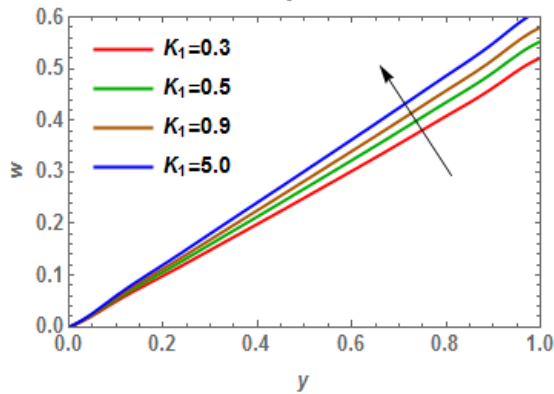
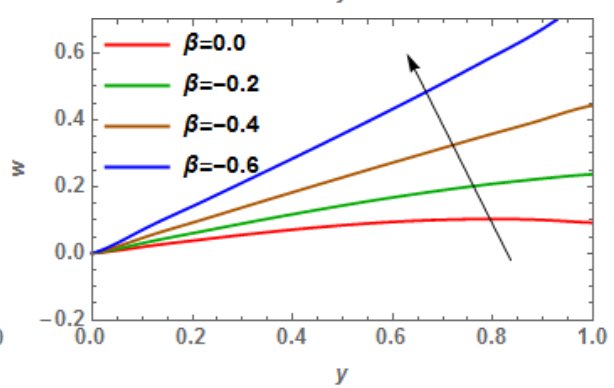
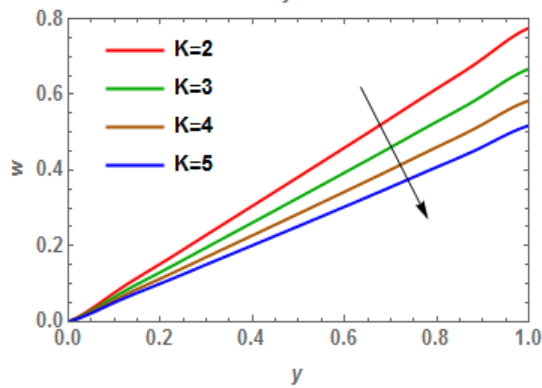
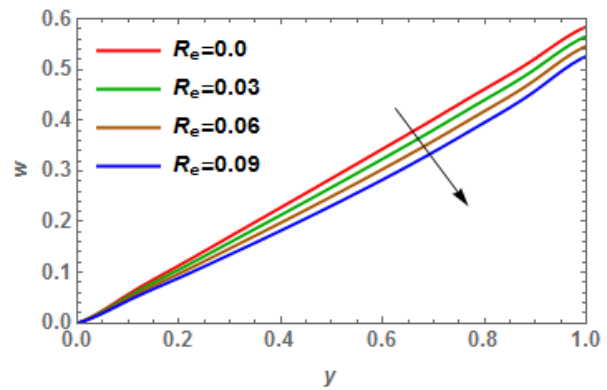
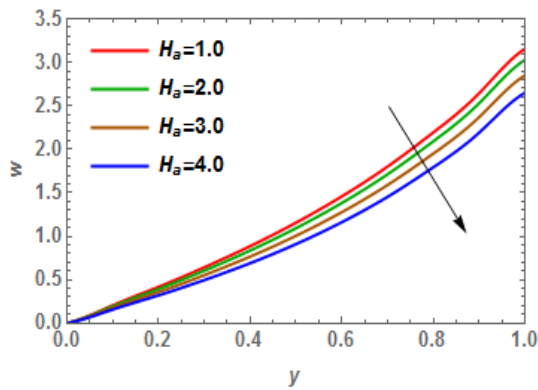
(c) $m = 30, \lambda = 10, \Theta = \frac{\Pi}{3}, R_e = 0.001, y = 0.9, \beta = -0.5, u_0 = 0.2, H_a = 1, \omega = 10, K_1 = 1$;

(d) $m = 30, \lambda = 10, \Theta = \frac{\Pi}{3}, K = 4, y = 0.9, \beta = -0.5, u_0 = 0.2, R_e = 0.001, \omega = 10, H_a = 1$;

(e) $H_a = 1, \lambda = 10, \Theta = \frac{\Pi}{3}, K = 4, y = 0.9, \beta = -0.5, u_0 = 0.2, R_e = 0.001, \omega = 10, K_1 = 2$;

(f) $m = 30, \lambda = 10, \Theta = \frac{\Pi}{3}, K = 4, y = 0.9, H_a = 1, u_0 = 0.2, R_e = 0.001, \omega = 10, K_1 = 1$;

(g) $m = 30, \lambda = 10, H_a = 1, K = 4, y = 0.9, \beta = -0.5, u_0 = 0.2, R_e = 0.001, \omega = 10, K_1 = 1$



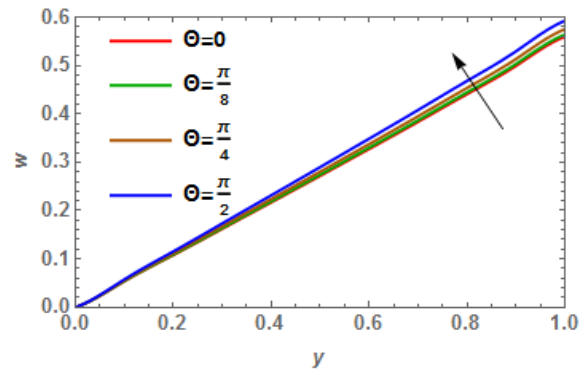


Figure 4(a-g). Microrotation profile with respect to y for.

(a) $m = 30, \lambda = 10, \Theta = \frac{\pi}{3}, K = 4, t = 0, \beta = -0.5, u_0 = 1, R_e = 0.001, \omega = 10, K_1 = 2$;

(b) $m = 3, \lambda = 10, \Theta = \frac{\pi}{3}, K = 4, t = 0.2, \beta = -0.5, u_0 = 0.2, H_a = 1, \omega = 10, K_1 = 1$;

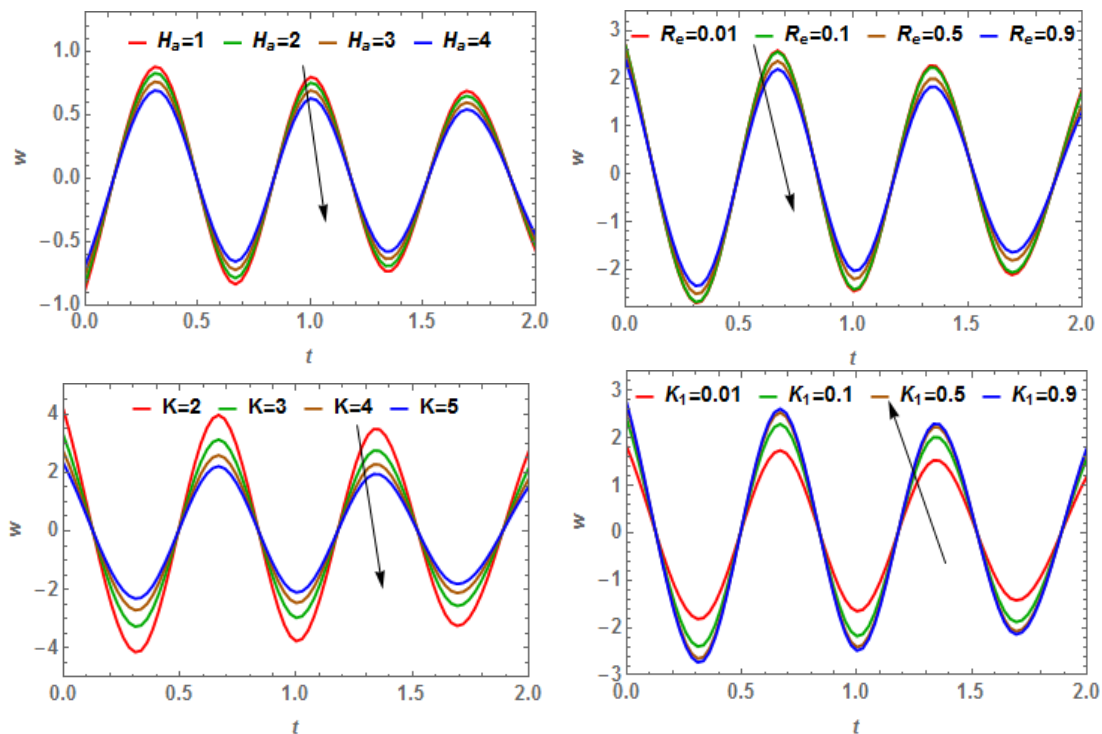
(c) $m = 3, \lambda = 10, \Theta = \frac{\pi}{3}, H_a = 1, t = 0.2, \beta = -0.5, u_0 = 0.2, R_e = 0.001, \omega = 10, K_1 = 1$;

(d) $m = 3, \lambda = 10, \Theta = \frac{\pi}{3}, K = 4, t = 0.2, H_a = 1, u_0 = 0.2, R_e = 0.001, \omega = 10, K_1 = 1$;

(e) $H_a = 1, \lambda = 10, \Theta = \frac{\pi}{3}, K = 4, t = 0.2, \beta = -0.5, u_0 = 0.2, R_e = 0.001, \omega = 10, K_1 = 2$;

(f) $m = 3, \lambda = 10, \Theta = \frac{\pi}{3}, K = 4, t = 0.2, \beta = -0.5, u_0 = 0.2, R_e = 0.001, \omega = 10, H_a = 1$;

(g) $m = 3, \lambda = 10, H_a = 1, K = 4, t = 0.2, \beta = -0.5, u_0 = 0.2, R_e = 0.001, \omega = 10, K_1 = 1$



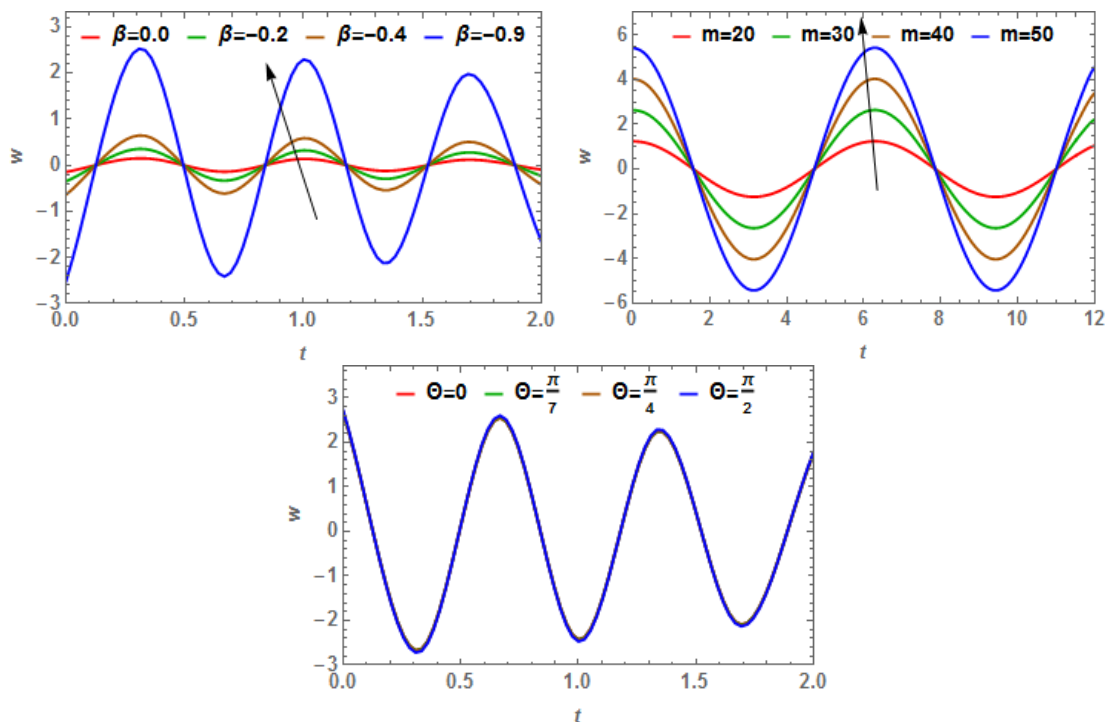
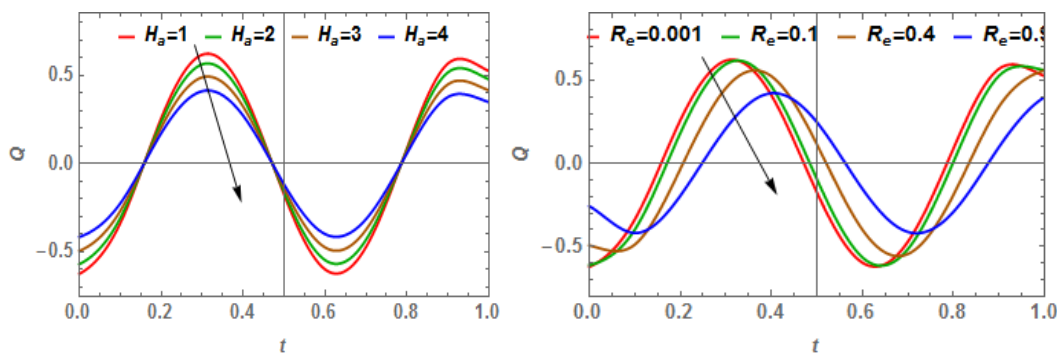


Figure 5(a-g). Microrotation profile with respect to t for.

- (a) $m = 5, \lambda = 10, \Theta = \frac{\pi}{3}, K = 4, y = 0.9, \beta = -0.5, u_0 = 0.2, R_e = 0.001, \omega = 10, K_1 = 2$;
- (b) $m = 30, \lambda = 10, \Theta = \frac{\pi}{3}, K = 4, H_a = 1, y = 0.9, \beta = -0.5, u_0 = 0.2, \omega = 10, K_1 = 1$;
- (c) $m = 30, \lambda = 10, \Theta = \frac{\pi}{3}, R_e = 0.001, y = 0.9, \beta = -0.5, u_0 = 0.2, H_a = 1, \omega = 10, K_1 = 1$;
- (d) $m = 30, \lambda = 10, \Theta = \frac{\pi}{3}, K = 4, y = 0.9, \beta = -0.5, u_0 = 0.2, R_e = 0.001, \omega = 10, H_a = 1$;
- (e) $m = 5, \lambda = 10, \Theta = \frac{\pi}{3}, K = 4, y = 0.9, H_a = 1, u_0 = 0.2, R_e = 0.001, \omega = 10, K_1 = 1$;
- (f) $H_a = 1, \lambda = 10, \Theta = \frac{\pi}{3}, K = 4, y = 0.9, \beta = -0.5, u_0 = 0.2, R_e = 0.001, \omega = 10, K_1 = 2$;
- (g) $m = 30, \lambda = 10, H_a = 1, K = 4, y = 0.9, \beta = -0.5, u_0 = 0.2, R_e = 0.001, \omega = 10, K_1 = 1$



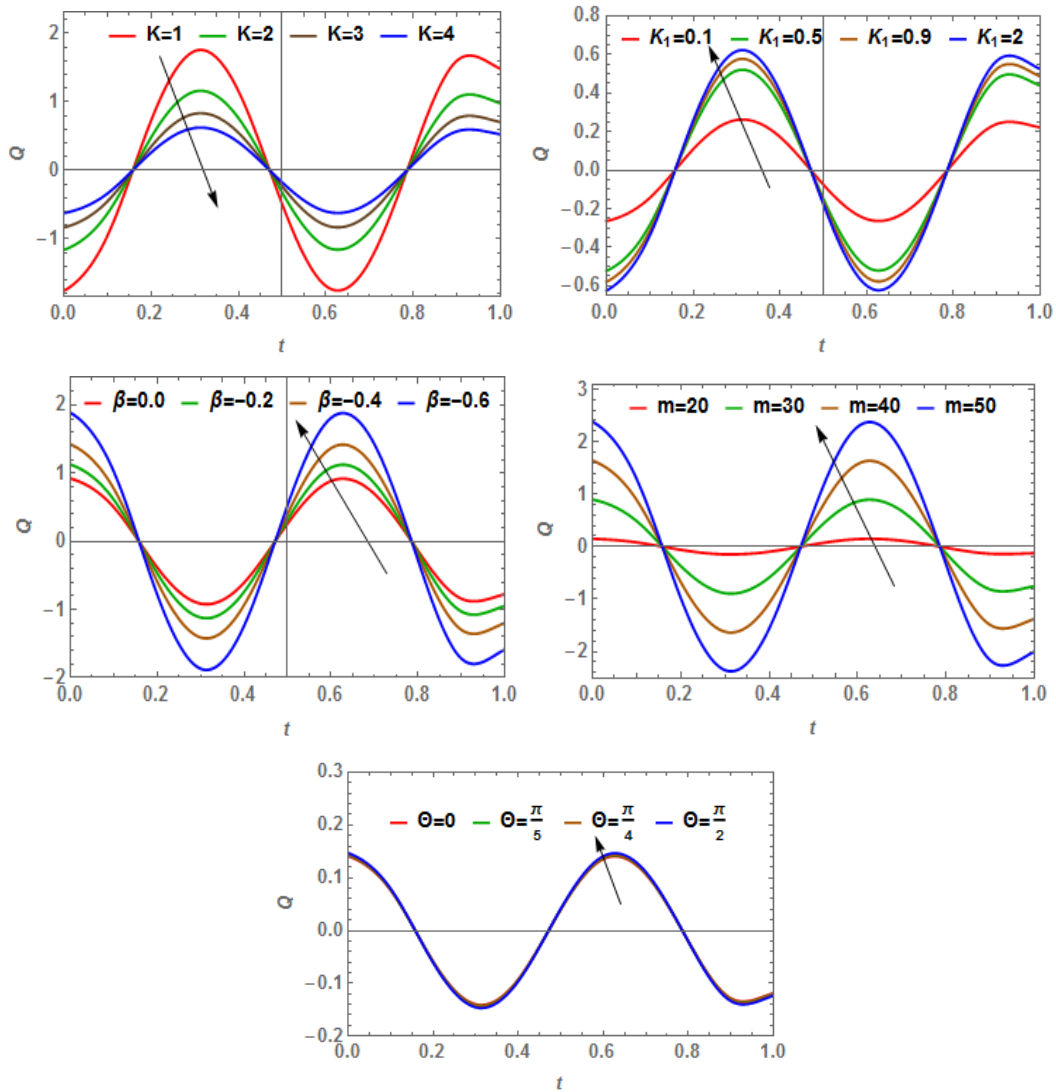


Figure 6(a-g). Variation of volumetric flow rate for

- (a) $m = 10, \lambda = 10, \Theta = \frac{\pi}{3}, K = 4, \beta = -0.5, u_0 = 0.2, R_e = 0.001, \omega = 10, K_1 = 2$;
- (b) $m = 10, \lambda = 10, \Theta = \frac{\pi}{3}, K = 4, H_a = 1, \beta = -0.5, u_0 = 0.2, \omega = 10, K_1 = 2$;
- (c) $m = 10, \lambda = 10, \Theta = \frac{\pi}{3}, R_e = 0.001, \beta = -0.5, u_0 = 0.2, H_a = 1, \omega = 10, K_1 = 2$;
- (d) $m = 10, \lambda = 10, \Theta = \frac{\pi}{3}, K = 4, \beta = -0.5, u_0 = 0.2, R_e = 0.001, \omega = 10, H_a = 1$;
- (e) $m = 20, \lambda = 10, \Theta = \frac{\pi}{3}, K = 4, H_a = 1, u_0 = 0.2, R_e = 0.001, \omega = 10, K_1 = 2$;
- (f) $H_a = 1, \lambda = 10, \Theta = \frac{\pi}{3}, K = 4, \beta = -0.5, u_0 = 0.2, R_e = 0.001, \omega = 10, K_1 = 2$;
- (g) $m = 20, \lambda = 10, H_a = 1, K = 4, \beta = -0.5, u_0 = 0.2, R_e = 0.001, \omega = 10, K_1 = 1$

5. CONCLUSION

A complete theoretic analysis has been considered here with the aim of investigating the characteristics of electroosmotically actuated micropolar fluid flow through microfluidic confinements bounded by two porous micro-parallel plates that are oscillating. The analytical solutions of the velocity and microrotation are derived by using the Debye-Huckel linear approximation. The numerical approximations presented in the previous section bear the potential of describing the electro-osmotic flow behavior of blood in the micro-circulatory system, when the system is under the influence of an external magnetic and electric field. These results are expected to be of immense interest to clinicians and bio-engineers. The main findings are summarized below.

1. Both the velocity and the microrotation of the microparticles decrease by increasing the value of Hartmann number.
2. The behavior of micropolar parameter and Hartmann number on the flow characteristics of the micropolar fluid is similar.
3. Both the velocity and the microrotation of the microparticles increase by increasing the Debye Huckel Parameter m .
4. By increasing the value of porous parameter, microrotation and volume flow rate increases.
5. Increasing values of inclination angle of the magnetic field enhances the velocity as well as the microrotation of the erythrocytes.
6. The volume flow rate increases by increasing the Debye Huckel parameter, porous parameter and the boundary parameter β .

REFERENCES

1. J. C. Misra, G. C. Shit, S. Chandra. Electro-osmotic flow of a viscoelastic fluid in a channel: Application to physiological fluid mechanics, *Applied Mathematics and Computation.*, 2011; 217(20): 7932-7939.
2. C. L. Rice, R. Whitehead. Electrokinetic flow in a narrow cylindrical capillary, *J. Phys. Chem.*, 1965; 69: 4017-4024.
3. Y. Kang, C. Yang, X. Huang. Dynamic aspects of electroosmotic flow in a cylindrical microcapillary, *Int. J. Eng. Sci.*, 2002; 40: 2203-2221.
4. J. C. Misra, S. Chandra. Electro-osmotic flow of a second-grade fluid in a porous microchannel subject to an AC electric field, *Journal of Hydrodynamics*, 2013; 25(2): 309-316.

5. J. C. Misra, A. Sinha. Electro-osmotic flow and heat transfer of a non-Newtonian fluid in a hydrophobic microchannel with Navier slip, *Journal of Hydrodynamics*, 2015; 27(5): 647-657.
6. W. Choi, S. W. Joo, G. Lim. Electroosmotic flows of viscoelastic fluids with asymmetric electrochemical boundary conditions, *Journal of Non-Newtonian Fluid Mechanics*, 187-188 (2012) 1-7.
7. A. MatÃ-ias, S. Sanchez, F. Mendez, O. Bautista. Influence of slip wall effect on a non-isothermal electro-osmotic flow of a viscoelastic fluid, *International Journal of Thermal Sciences*, 201598: 352-363.
8. A. M. Afonso, M.A. Alves, F.T. Pinho. Analytical solution of two-fluid electro-osmotic flows of viscoelastic fluids, *Journal of Colloid and Interface Science*, 2013; 395: 277-286.
9. Cunlu Zhao, Chun Yang. Exact solutions for electro-osmotic flow of viscoelastic fluids in rectangular micro-channels. *Applied Mathematics and Computation*, 2009; 211: 502-509.
10. Cunlu Zhao, Chun Yang. An exact solution for electroosmosis of non Newtonian fluids in microchannels, *Journal of Non-Newtonian Fluid Mechanics*, 2011; 166: 1076-1079.
11. G.H. Tang, X.F. Li, Y.L. He, W.Q. Tao. Electroosmotic flow of non-Newtonian fluid in microchannels, *J. Non-Newtonian Fluid Mech.*, 2009; 157: 133-137.
12. G.H. Tang, P.X. Ye, W.Q. Tao. Electroviscous effect on non-Newtonian fluid flow in microchannels, *J. Non-Newtonian Fluid Mech.*, 2010; 165: 435-440.
13. Simeng Chen, Xinting He, Volfango Bertola, Moran Wang. Electro-osmosis of non-Newtonian fluids in porous media using lattice Poissonâ€“Boltzmann method, *Journal of Colloid and Interface Science.*, 2014; 436: 186-193.
14. A. M. Afonso,Â·M. A. Alves, F. T. Pinho. Electro-osmotic flow of viscoelastic fluids in microchannels under asymmetric zeta potentials, *J Eng Math*, 2011; 71: 15-30.
15. A. Sadeghi, Y. Kazemi, M.H. Saidi. Joule heating effects in electrokinetically driven flow through rectangular microchannels: an analytical approach, *Nanoscale and Microscale Thermophysical Engineering*, 2013; 17: 173-193.
16. M. A. Vakili, M. H. Saidi, A. Sadeghi, Thermal transport characteristics pertinent to electrokinetic flow of power-law fluids in rectangular microchannels, *International Journal of Thermal Sciences.*, 2014; 79: 76-89.
17. G.C. Shit, A. Mondal, A. Sinha, P.K. Kundu, Effects of slip velocity on rotating electro-osmotic flow in a slowly varying micro-channel, *Colloids and Surfaces A: Physico chem. Eng. Aspects.*, 2016; 489: 249-255.
18. M. Mondal, R.P. Misra and S. De, Combined electroosmotic and pressure driven flow in

- a microchannel at high zeta potential and overlapping electrical double layer, *International Journal of Thermal Sciences.*, 2014; 86: 48-59.
19. L. Wang, Y. Jain, Q. Liu, F. Li and L. Chang, Electromagnetohydrodynamic flow and heat transfer of third grade fluids between two microparallel plates, *Colloids and Surfaces A: Physicochem. Eng. Aspects*, 2016; 494: 87-94.
 20. A. C. Eringen. Simple microfluids, *International Journal of Engineering Science*, 1964; 2: 205-217.
 21. A. C. Eringen. Theory of micropolar fluids. *Journal of Applied Mathematics and Mechanics*, 1965; 16: 1-18.
 22. A. C. Eringen. *Microcontinuum field theories II: Fluent media [M]*. New York, USA: Springer, 2001.
 23. A. A. Siddiqui, A. Lakhtakia. Steady electroosmotic flow of a micropolar fluid in a microchannel[J]. *Proceedings the Royal of Society A*, 2009; 465: 501-522.
 24. A. A. Siddiqui, A. Lakhtakia. Non-steady electro-osmotic flow of a micropolar fluid in a microchannel[J]. *Journal of Physics A: Mathematical and Theoretical*, 2009; 42(35): 2203-2211.
 25. J. C. Misra, S. Chandra. Electro-osmotically actuated oscillatory flow of a physiological fluid on a porous microchannel subject to an external AC electric field having dissimilar frequencies. *Cent. Eur. J. Phys.*, 2014; 12(4): 274-285.
 26. J. C. Misra, S. Chandra. H. Herwig. Flow of a micropolar fluid in a micro-channel under the action of an alternating electric field: Estimates of flow in bio-fluidic devices. *Journal of hydrodynamics*, 2015; 27(3): 350-358.
 27. Zhaodong Ding, Yongjun Jian, Liangui Yang. Time periodic electroosmotic flow of micropolar fluids through microparallel channel. *Appl. Math. Mech. Engl. Ed.* DOI 10.1007/s10483-016-2081-6
 28. A. A. Siddiqui, A. Lakhtakia. Debye-Huckel solution for steady electro-osmotic flow of micropolar fluid in cylindrical microcapillary. *Applied Mathematics and Mechanics (English Edition)*, 2013; 34(11): 1305-1326.
 29. I. Papautsky, J. Brazzle, T. Ameel, A. B. Frazier. Laminar fluid behavior in microchannels using micropolar fluid theory. *Sensors and Actuators, A: Physical*, 1999; 73: 101-108.
 30. E. Magyari, I. Pop, P. P. Valkó. Stoke's first problem for micropolar fluids. *Fluid Dynamics Research*, 2010; 42: 025503.
 31. T. Ariman, M. A. Turk, N. D. Sylvester. *Microcontinuum fluid mechanics – a review.*

- International Journal of Engineering Science, 1973; 11: 905-930.
32. T. Ariman, M. A. Turk, N. D. Sylvester. Application of microcontinuum fluid mechanics. International Journal of Engineering Science, 1974; 12: 273-293.
33. V. K. Stokes. Theories of Fluids with Microstructures, Springer, New York., 1984.
34. G. Lukaszewicz. Micropolar Fluids: Theory and Application, Birkh user, Basel., 1999.
35. Ajaz Ahmad Dar, K. Elangovan. Influence of an inclined magnetic field and rotation on the peristaltic flow of a micropolar fluid in an inclined channel. Hindawi Publishing Corporation, New Journal of Science, Volume 2016, Article ID 5717542, 14 pages <http://dx.doi.org/10.1155/2016/5717542>
36. D. Li. Electrokinetics in Microfluidics, Elsevier, London., 2004.